Inorganic Chemistry

Article

pubs.acs.org/IC

The Mechanism of Homogeneous CO_2 Reduction by Ni(cyclam): Product Selectivity, Concerted Proton–Electron Transfer and C–O Bond Cleavage

Jinshuai Song, Eric L. Klein, Frank Neese, and Shengfa Ye*

Max-Planck Institute for Chemical Energy Conversion, Stiftstrasse 34–36, D-45470 Mülheim an der Ruhr, Germany

Supporting Information

ABSTRACT: Homogeneous CO_2 reduction catalyzed by $[Ni^I(cyclam)]^+$ (cyclam = 1,4,8,11-tetraazacyclotetradecane) exhibits high efficiency and selectivity yielding CO only at a relatively low overpotential. In this work, a density functional theory study of the reaction mechanism is presented. Earlier experiments have revealed that the same reaction occurring on mercury surfaces generates a mixture of CO and formate. According to the proposed mechanism, an η^1-CO_2 adduct is the precursor for CO evolution, whereas formate is obtained from an η^1-OCO adduct. Our calculations show that generation of the η^1-CO_2 adduct is energetically favored by ~14.0 kcal/mol relative to that of the η^1-OCO complex, thus rationalizing the product selectivity observed experimentally. Binding of η^1-CO_2 to Ni^I only leads to partial electron transfer from the metal center to CO_2. Hence, further CO_2 functionalization likely proceeds via an outer-sphere electron-transfer mechanism, for which concerted proton coupled electron transfer (PCET) is calculated to be the most feasible route. Final C–O bond cleavage involves rather low barriers in the presence of H_3O^+ and H_2CO_3 and is therefore essentially concerted with the preceding PCET. As a result, the entire reaction mechanism can be described as concerted proton–electron transfer and C–O bond cleavage. On the basis of the theoretical results, the limitations of the catalytic activity of Ni(cyclam) are discussed, which sheds light on future design of more efficient catalysts.

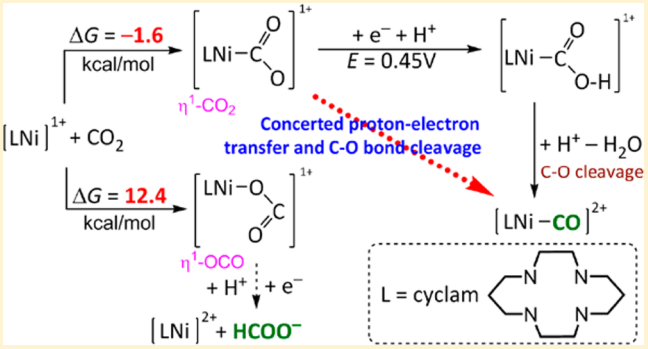

INTRODUCTION

Carbon dioxide is abundant in the atmosphere and reached a peak concentration of about 396 ppm last year.[1] It is a major greenhouse gas that contributes significantly to global warming, while it is also a cheap and nontoxic C1 feedstock that can be used for the production of value-added fine chemicals.[2] Because of its high stability and nonpolar nature, CO_2 functionalization typically requires high energy input in conjunction with appropriate catalysts,[3] thereby posing a formidable, yet worthwhile challenge for chemists.

Electrochemical CO_2 transformation has been intensively explored over the course of the last four decades.[3,4] However, direct electrochemical reduction of CO_2 on metal electrodes generally occurs at considerably negative potentials, and products and/or intermediates may poison metal surfaces.[4d] Using mercury electrodes, CO_2 conversion mediated by redox-active catalysts such as transition metal complexes often displays high turnover numbers with the common products being CO, formate, and oxalate.[4a,5] Of investigated reactions, CO_2 reduction catalyzed by Ni(cyclam) (cyclam = 1,4,8,11-tetraazacyclotetradecane) is particularly interesting since the reaction exhibits high efficiency at a relatively low overpotential.[4c,ag] Early experiments[6] proved that $[Ni(cyclam)]^+$, generated by 1 electron (e) reduction of precatalyst $[Ni^{II}(cyclam)]^{2+}$, is the catalytically active species. Interestingly, CO_2 is exclusively reduced to CO in water. By contrast, both CO and formate are obtained in wet dimethylformamide (DMF) with the CO/formate ratio ranging from 1:3 to 4:3 depending on the applied reduction potentials. In aqueous solution, reduction of H_2O to H_2 is expected to be a side reaction. However, $[Ni(H)(cyclam)]^{2+}$, the proposed precursor for H_2 evolution, cannot form under the experimental condition of pH ≈ 4, because the pK_a value of $[Ni(H)(cyclam)]^{2+}$ was determined experimentally to be ~1.8.[7] In addition, the concentration of CO_2 in the reaction solution is at least 2 orders of magnitude higher than that of H^+, and thus CO_2 coordination to $[Ni(cyclam)]^+$ is favored. Furthermore, mercury appears to be indispensable for CO_2 reduction by $[Ni(cyclam)]^+$, as the reaction has been identified to take place predominantly at the mercury surface.[6b,8] In search for more environmentally benign catalysts, Kubiak and co-workers recently reported that this reaction can proceed in a homogeneous fashion using an inert glassy carbon electrode. At −1.21 V versus the normal hydrogen electrode (NHE), the primary product was found to be CO with 90% Faraday efficiency, and no H_2 or formate was detected.[9]

Received: April 8, 2014
Published: June 24, 2014

   dx.doi.org/10.1021/ic500829p | Inorg. Chem. 2014, 53, 7500–7507

It is most likely that CO_2 reduction by $[Ni^I(cyclam)]^+$ proceeds via an inner-sphere electron-transfer mechanism, because the 1 e reduction potential of CO_2 to $CO_2^{\bullet-}$ is much more negative (−1.90 V vs NHE in water[10]) than the experimentally applied potentials.[11] Thus, the formation of CO_2 adduct is undoubtedly the initial step of the catalytic cycle. However, $[Ni(CO_2)(cyclam)]^+$ has not been trapped in high concentrations, and hence extensive spectroscopic characterizations have not been possible yet. In fact, three different binding modes of CO_2, namely, η^1-CO_2, η^1-OCO, and η^2-CO_2, have been observed in the crystal structures of a large range of mononuclear transition metal CO_2 adducts.[12] With regard to nickel complexes specifically, only side-on η^2-CO_2 structures have been reported to date.[12f−i] Most theoretical studies have focused on the geometric and electronic structures of CO_2 complexes with low-coordinate Ni centers, and the results revealed that both η^2-CO_2 and η^1-CO_2 are energetically favored coordination modes.[13] For Ni(cyclam), Sakaki reported that CO_2 can bind to $[Ni^IF(NH_3)]^0$ yielding a stable η^1-CO_2 species, whereas the corresponding η^2-CO_2 adduct is significantly less stable.[14] In recent theoretical studies of the CO_2 adduct of $[Ni(cyclam)]^+$,[4b,9] the η^1-CO_2 binding mode was assumed, and no comparison between different coordination modes of CO_2 was made. To our knowledge, no computational investigation on the interaction of η^1-OCO with four-coordinate nickel centers has been published.

In the 1980s, Collin et al. proposed a catalytic mechanism (summarized in Scheme 1) to explain how both CO and formate can be formed on mercury.[6a] It was suggested that initially CO_2 binds to $[Ni^I(cyclam)]^+$ in the three possible coordination modes, which can interconvert to each other.[12a,b] After formation of a CO_2 adduct, the reaction pathways resulting in either CO or formate bifurcate. The η^1-CO_2 species may accept an electron and a proton to yield the carboxylate intermediate $[Ni(C(O)OH)(cyclam)]^+$ that subsequently undergoes heterolytic C−O bond cleavage to generate CO in the presence of a proton. The η^1-OCO complex may directly transform into a nickel formate species $[Ni(OCOH)(cyclam)]^+$ via uptake of an electron and a proton.

Scheme 1. Proposed Mechanism for CO_2 Reduction by Ni(cyclam)[6a]

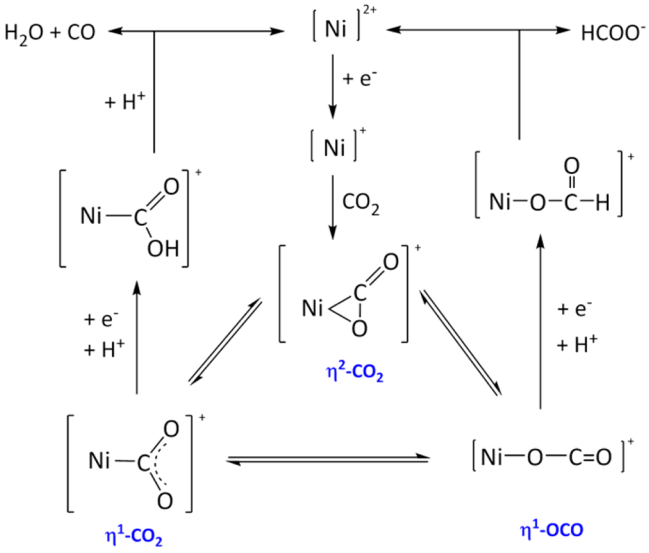

Although the CO_2 reduction by $[Ni^I(cyclam)]^+$ has been studied for over 30 years, the mechanistic details have not been well understood yet. Related work on the CO_2 activation by Fe(porphyrin)[15] and Pd(triphosphine) complexes[16] has demonstrated that the reactions are accelerated in the presence of Brönsted or Lewis acids. This experimental finding suggests the role of acids in promoting electron transfer from the metal center to CO_2. Thus, the reaction following the formation of the CO_2 adduct might proceed via proton-coupled electron transfer (PCET)[4u,17] or metal ion-coupled electron transfer (MCET).[4u] The crystal structure of a $Co^I(\eta^1$-$CO_2)$ species with a cyclam-like macrocyclic ligand points to a similar reaction mechanism for the CO_2 functionalization by $[Ni^I(cyclam)]^+$. The complex is crystallized as a bimetallic form[18] in which one Co center binds to the central C atom of CO_2 and the other acts as a Lewis acid to interact with the distal O atom. Furthermore, Brönsted acids have been experimentally and computationally identified to be essential for CO_2 reduction by $M(bpy)(CO)_3X$ (M = Mn, Re; X = anionic ligand or solvent)[19] and $Mn(NHC)(CO)_3Br$ (NHC = N-heterocyclic carbene).[20]

In this work, a computational study of the reaction mechanism of the homogeneous CO_2 reduction by Ni(cyclam) is presented. In particular, the interaction of the Ni center with CO_2 in various coordination modes and the subsequent CO_2 reduction step are analyzed in detail.

COMPUTATIONAL SETUP

All calculations were performed using the ORCA program package.[21] The hybrid density functional B3LYP[22] was employed for geometry optimizations and frequency calculations. Relativistic effects were treated using the zeroth-order regular approximation (ZORA)[23] for which the ZORA-def2-TZVP[24] basis set was used. Calculations were accelerated with the resolution of identity and chain of sphere (RIJCOSX) approximations[25] in conjunction with the def2-TZVP/J auxiliary basis set.[26] Dispersion effects were accounted for using the semiempirical van der Waals corrections by Grimme[27] implemented in ORCA. All geometries were fully optimized without symmetry constraints. Harmonic vibrational frequencies were computed to verify the nature of stationary points. The minimum energy structures reported in this Paper have positive eigenvalues of the Hessian matrix, whereas the transition states have only one negative eigenvalue. The zero-point energies, thermal corrections, and entropy terms for the optimized geometries were obtained from the frequency calculations. In the case of combination reactions in gas phase, the reference point to calculate entropy terms of Gibbs free energies can be chosen to be infinitely separated reactants. However, for reactions in solution this approximation can lead to an error of over 10 kcal/mol based on our earlier work,[28] because in solution only when all reactants enter into the same solvent cage can the reaction easily occur. Thus, we can reasonably assume a series of pre-equilibriums[29] between reactants and calculate reaction barriers and free energies with respect to the lowest-energy reaction complex, in which reactants weakly interact with each other. Nevertheless, this approximation may slightly underestimate the entropy contributions as the individual translational entropy of each reactant is completely neglected. To approach the basis set limit, final single-point energies were computed with the large and flexible def2-TZVPP[30] basis set for all elements.

Calculations of redox potentials and pK_a values are based on the widely accepted thermodynamic cycles (for details, see the Supporting Information). Solvation energies were estimated at the optimized geometries in the gas phase using the conductor-like screening model (COSMO).[31] To simulate the solvation effect of the mixed solvent employed in the experiments (water/acetonitrile = 1:4), the dielectric constant ε was set to 45.36.[32] For redox potential calculations, the relative redox potential was calculated with respect to the NHE, for which a shift of −4.48 V (the NHE value in acetonitrile) was used.[33] For pK_a calculations, the gas phase standard Gibbs free energy of

dx.doi.org/10.1021/ic500829p | Inorg. Chem. 2014, 53, 7500−7507

formation of a proton was set to −6.28 kcal/mol.[34] The solvation energy of a proton in the mixed solvent is unknown, so the value in acetonitrile was used approximately (−260.2 kcal/mol).[33]

To calibrate our computational setup, we calculated the 1 e reduction potentials of $[Ni(cyclam)]^{2+}$, as well as the derivatives 1,8-dimethylcyclam (DMC) and 1,4,8,11-tetramethylcyclam (TMC). Our theoretical results (Table 1) show reasonable agreement with experiment within an error of less than 200 mV.[35] This type of agreement is roughly as good as can be expected for the employed methodology. Note that the effective errors of the relative reduction potentials should be smaller than 200 mV due to error cancellation. In addition, the reduction potentials of this testing set were also computed using the COSMO-RS solvation model.[36] However, the results show a slightly larger deviation of ∼250 mV (Supporting Information, Table S1). Therefore, the COSMO solvation model was employed for the following mechanistic study.

Table 1. Comparison of Calculated and Experimental Reduction Potentials ($E°$) for $[Ni(cyclam)]^{2+/+}$, $[Ni(DMC)]^{2+/+}$ and $[Ni(TMC)]^{2+/+}$

ligand	$E°$ (calc)	$E°$ (exp)[9]
trans-I-cyclam	−1.07	−1.23
trans-III-cyclam	−1.12	−1.23
DMC	−1.01	−1.03
TMC	−0.71	−0.65

RESULTS AND DISCUSSION

2.1. CO_2 Adducts. As discussed in the Introduction, the binding of CO_2 to $[Ni^I(cyclam)]^+$ (^{2}**1**, the superscript is used to denote the spin multiplicity of a given species) initiates CO_2 reduction. Consequently, before entering into a meaningful discussion of the reaction mechanism, the possible geometric and electronic structures of the CO_2 adduct must be analyzed in detail.

Our calculations confirm the experimental finding that ^{2}**1** is the catalytically active species toward CO_2 reduction in that all attempts to locate a local minimum corresponding to the CO_2 adduct of $[Ni(cyclam)]^{2+}$ (^{1}**0**) lead to CO_2 dissociation. In addition to the distinct binding modes of CO_2, a second layer of complexity arises from different cyclam conformations.[37] Earlier experiments have revealed that at 25 °C there is 15% *trans*-I and 85% *trans*-III for ^{1}**0** in aqueous solution (Scheme 2).[38] Our calculations suggest that both conformations are also dominant forms for ^{2}**1** with other conformations lying at least 7 kcal/mol higher in energy (Supporting Information, Table S2). Thus, the three CO_2 binding modes and the two cyclam conformations were taken into account in modeling of the CO_2 adduct. Of the two cyclam conformations, *trans*-I cyclam affords marginally more stable CO_2 complexes regardless of the CO_2 coordination modes (Table 2). This may be ascribed to the four H_N atoms in *trans*-I cyclam that are geometrically accessible for hydrogen bonding with CO_2 relative to the two H_N atoms in *trans*-III (Supporting Information, Figure S1).[4b,9] Since very similar results are found for both *trans*-I and *trans*-III CO_2 complexes, documented below are the results of the *trans*-I species, and those of *trans*-III, which are summarized in the Supporting Information (Figure S3). In contrast to the cyclam conformations, the distinct CO_2 binding modes have a significant influence on the relative stability of the investigated CO_2 adducts. During the course of the geometry optimizations, the initial η^2-CO_2 structures invariably rearranged to $[Ni^I(\eta^1\text{-}CO_2)(cyclam)]^+$ (^{2}**2**) (Figure 1), indicating that the latter binding mode is far more energetically favored.[39] Likewise, the η^1-OCO adduct ($[Ni^I(\eta^1\text{-}OCO)(cyclam)]^+$, ^{2}**2′**) is destabilized by ∼14 kcal/mol in energy compared to ^{2}**2**. More importantly, the formation of the η^1-CO_2 adduct is essentially thermoneutral, consistent with the reported measurement in water (−1.6 kcal/mol).[7] By contrast, the binding process yielding the η^1-OCO complex is highly endergonic by 12.4 kcal/mol. Therefore, the reaction pathway leading to the formation of formate is insignificant at this stage, and ^{2}**2** is the only viable species to participate in the actual catalytic cycle. Our theoretical results suggest that once ^{2}**2′** could form, the subsequent reaction yielding formate would be facile (Supporting Information, Figure S5). To address the question about why both CO and formate can be generated using mercury electrodes, the intrinsically active species on mercury must be identified, because it has been reported that the adsorption of Ni(cyclam) on mercury induces a reconfiguration of the cyclam ligand and hence a change the reactivity of Ni(cyclam).[8b] Furthermore, our calculations suggest that $[Ni(H)(cyclam)]^{2+}$ is indeed an efficient precursor for H_2 evolution (Supporting Information, Figure S6). However, this species cannot form under the experimental conditions.

Relative to the linear structure of noncoordinated CO_2, the most remarkable geometric feature of ^{2}**2** and ^{2}**2′** is the bending of the coordinated CO_2 ligand. Moreover, the C−O bonds of CO_2 are considerably elongated upon CO_2 coordination to the Ni center (Table 2). Specially, the computed C−O distances in ^{2}**2** are in between those for CO_2^0 and $CO_2^{\bullet-}$, whereas the C−O distances in ^{2}**2′** match those found for $CO_2^{\bullet-}$ closely. As shown in Figure 1, ^{2}**2** features moderate π backdonation from the doubly occupied Ni−d_{z^2} electron-donating orbital (EDO) into the vacant CO_2 π_{ip}* (ip = in-plane) electron-accepting orbital (EAO).[40] This π backdonation interaction can be viewed as metal-to-ligand electron transfer. This interaction is stronger in the spin-down manifold, because the spin-polarization substantially stabilizes the spin-up Ni−d_{z^2} orbital, rendering it inactive as an EDO. Molecular orbital (MO) analysis shows that the electronic structure of ^{2}**2** is best described as a

Scheme 2. *Trans*-I and *trans*-III Nickel Cyclam Conformations

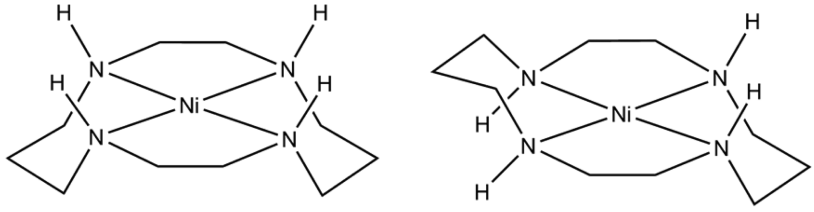

trans-I(*R*,*S*,*R*,*S*) *trans*-III(*S*,*S*,*R*,*R*)

dx.doi.org/10.1021/ic500829p | *Inorg. Chem.* 2014, 53, 7500−7507

Table 2. Comparison of Binding Parameters and Geometries of CO_2 Adducts

		binding free energies (ΔG, kcal/mol)	relative free energy (kcal/mol)	Ni–X (Å)	C–O (Å)	C–O (Å)	O–C–O (deg)
^{2}**2** (X = C)	*trans*-I	−1.6	0.0	2.046	1.212	1.211	142.9
	trans-III	2.7	1.2	2.091	1.212	1.211	142.2
^{2}**2′** (X = O)	*trans*-I	12.4	13.9	2.153	1.236	1.215	138.2
	trans-III	13.7	12.2	2.062	1.242	1.216	137.1
free CO_2					1.160	1.160	180.0
free $CO_2^{\bullet-}$					1.237	1.237	135.4

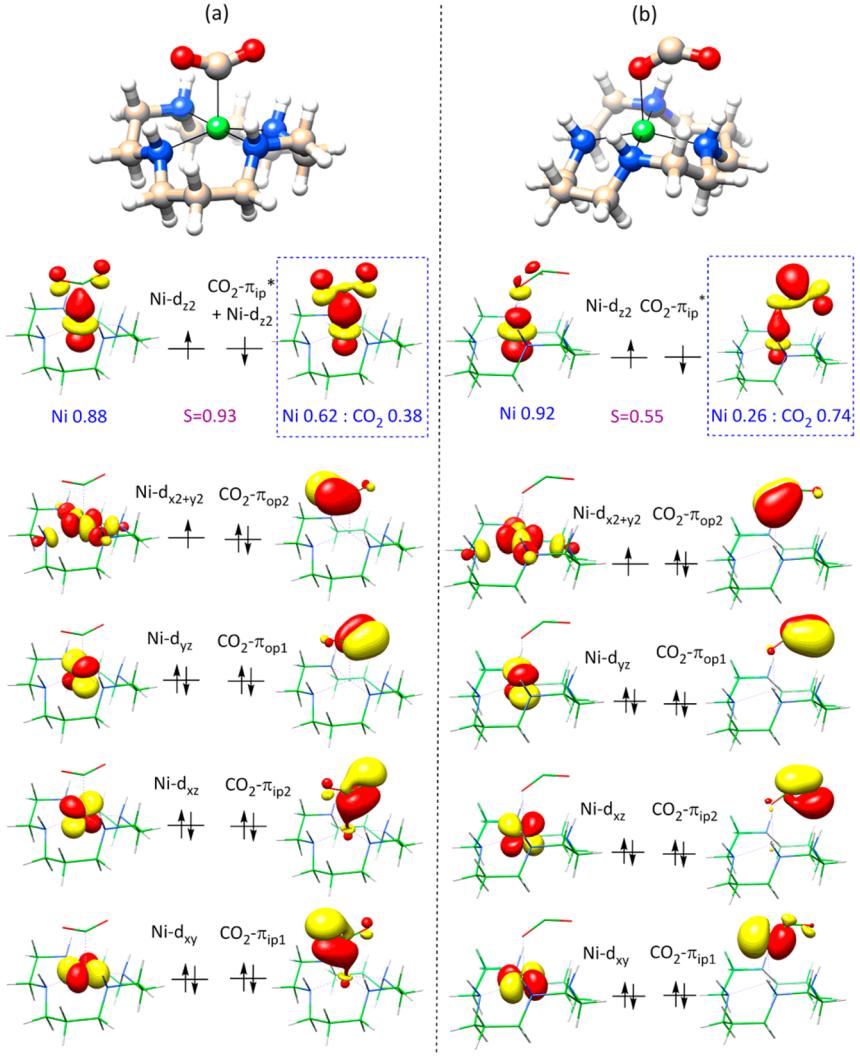

Figure 1. Optimized geometries and MO diagrams of ^{2}**2** (a) and ^{2}**2′** (b).

resonance structure between $Ni^I–CO_2^0$ and $Ni^{II}–CO_2^{\bullet-}$, in line with the C–O bond lengths calculated for ^{2}**2**. This implies that the first electron reduction of CO_2 is partially accomplished at this stage. Conversely, ^{2}**2′** contains a high-spin Ni^{II} center that is antiferromagnetically coupled to a $CO_2^{\bullet-}$ radical ligand (Figure 1), suggesting that the electron transfer is nearly complete. Among the d manifold of Ni^I, the d_{z^2}-based MO functions as the optimal EDO,[39] because this orbital has higher energy than the essentially nonbonding t_{2g}-derived d orbitals and can interact with CO_2 without significant steric hindrance.[39] The d_{z^2}-centered MO overlaps much more efficiently with the carbon lobe of the EAO than do the oxygen lobes, because in the EAO the contributions from the carbon p orbitals have higher weight than those of the terminal oxygen p orbitals (Figure 2). This polarization becomes more pronounced as CO_2 bends. More importantly, the bending of the CO_2 ligand lowers the energy of the EAO, hence enhancing its electron accepting ability. Thus, the more favorable Ni–CO_2 interaction leads to stronger stabilization of ^{2}**2** compared to ^{2}**2′**, and ^{2}**2′** involves the larger promotion energy resulting from the higher degree of the electron transfer from Ni^I to CO_2. These two factors together might rationalize the different binding energies calculated for ^{2}**2** and ^{2}**2′** (Table 2), as the entropy contributions are nearly identical for both species.

2.2. The Second Electron Reduction of CO_2 and Subsequent Heterolytic C–O Bond Cleavage. As implied by the electronic structure of ^{2}**2**, direct 2 e transfer from Ni^I to CO_2 is impossible, suggesting that further CO_2 reduction

dx.doi.org/10.1021/ic500829p | Inorg. Chem. 2014, 53, 7500–7507

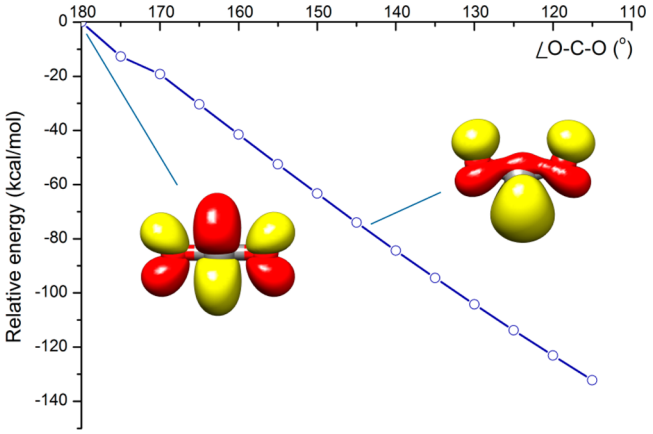

Figure 2. Evolution of the CO_2 π_{ip}* orbital as a function of the O−C−O angle.

requires an additional electron donor and likely proceeds via an outer-sphere electron-transfer mechanism. Compound **3**, which is the 1 e reduced form of ^{2}**2**, is theoretically predicted to possess a triplet ground state with a singlet state lying 18.2 kcal/mol higher in energy, and hence ^{1}**3** will not be discussed in the following. Direct 1 e reduction of ^{2}**2** to give ^{3}**3** is found to be extremely endergonic by as much as 37.0 kcal/mol (Scheme 3). This leads to a calculated reduction potential of −1.98 V, which is far more negative than the experimentally applied potential (−1.21 V). Therefore, PCET is likely to be operative in the further reaction as discussed in the Introduction. Moreover, direct protonation of ^{2}**2** to generate ^{2}**4** cannot easily occur because this reaction is also highly endergonic by 10.6 kcal/mol with H_3O^+, the strongest proton donor in solution. Congruent with this, the computed pK_a value of compound ^{2}**4** (−12.3), which is the conjugate acid of compound ^{2}**2**, is considerably lower than pH ≈ 4 at which the experiments were performed. Taken together, concerted PCET presents the most feasible pathway for the further reduction of CO_2 since both steps (^{2}**2** → ^{3}**3** and ^{2}**2** → ^{2}**4**) are strongly endergonic. Under the experimental conditions, the concentrations of the possible proton sources are computed as follows: $[H_3O^+]$ = 0.15 mM; $[H_2CO_3]$ = 0.09 mM; $[H_2O]$ = 11.1 M (for details, see the Supporting Information). Using the Nernst equation, the influence of the different concentrations of the proton sources on the reduction potentials can be estimated. The calculated reduction potentials for the concerted PCET transforming ^{2}**2** into ^{3}**5** are 0.41 V, −0.89 V, and −1.91 V using H_3O^+, H_2CO_3,

Scheme 3. Proposed Reaction Mechanism of CO Formation[a]

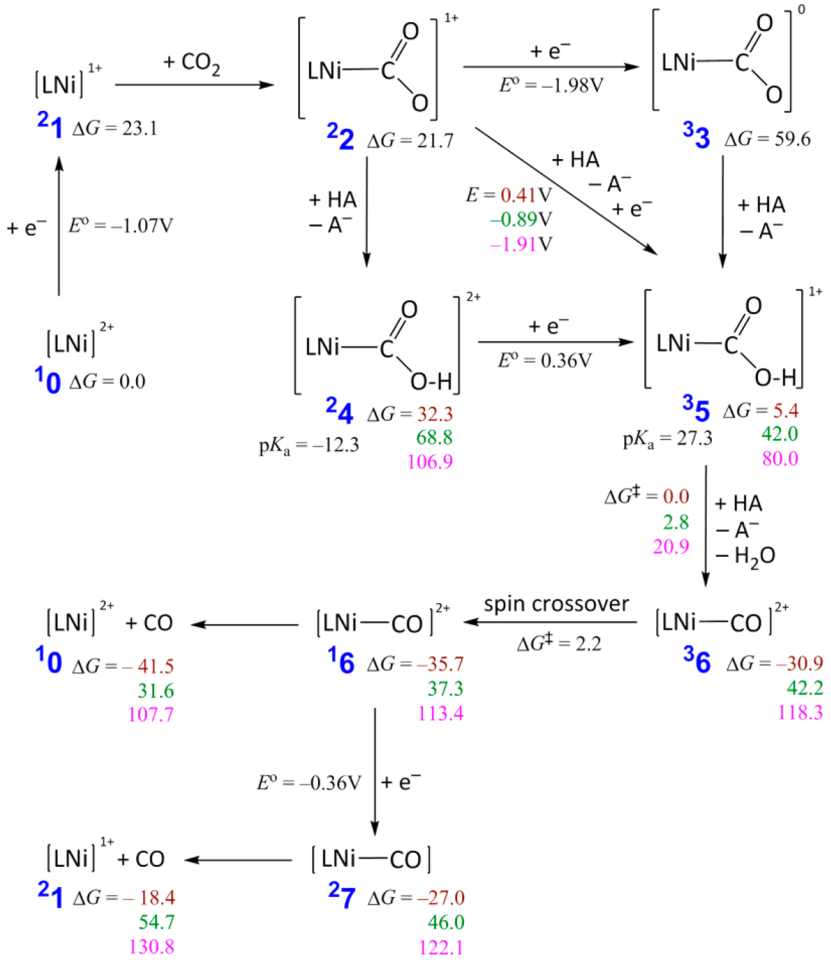

[a]Using H_3O^+ (brown), H_2CO_3 (green), and H_2O (magenta) as proton sources. Calculated pK_a values, the standard reduction potentials ($E°$), the actual reduction potentials of the concerted PCET (E), and relative Gibbs free energies (ΔG, kcal/mol) are given for each step. L represents *trans*-I cyclam.

dx.doi.org/10.1021/ic500829p | *Inorg. Chem.* 2014, 53, 7500−7507

and H_2O as the proton sources, respectively (see the Supporting Information). H_2CO_3 is an efficient proton donor; however, its concentration is much lower than those of H_2O and CO_2 (34 mM), and we thus tested the reaction of ^{2}**2** + H_2O + CO_2 + e^- → ^{3}**5** + HCO_3^-. The computed reduction potential of −1.37 V is slightly more negative than the experimentally applied potential within the limit of the computational uncertainty, which nevertheless suggests the less-important role of H_2O + CO_2 compared to H_2CO_3. Therefore, the reaction following the formation of the CO_2 adduct progresses via the concerted PCET for which H_3O^+ or H_2CO_3 may serve as the proton donor.

Our calculations predict a triplet ground state for **5**, which is 14.4 kcal/mol lower in energy than the lowest-energy singlet state. As shown in Figure 3, ^{3}**5** consists of a high-spin Ni^{II}

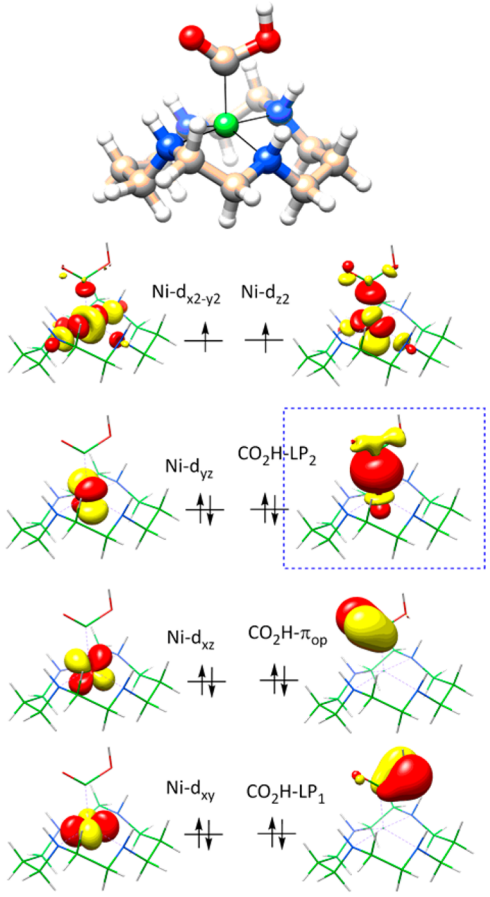

Figure 3. Optimized geometry and MO diagrams of intermediate ^{3}**5**.

center bound to a carboxylate anion $^-CO_2H$ (Ni^{II}–$^-CO_2H$). Consistent with this electronic structure description, one of the C−O bonds elongates to 1.386 Å, falling within the typical range of a C−O single bond, while the other C−O bond remains essentially as a double bond, evidenced by its bond length (1.224 Å) similar to that calculated for ^{2}**2**. The computed Meyer bond orders further corroborate this interpretation (1.0 for the former C−O bond and 1.7 for the latter). More importantly, the lone pair of the central carbon atom in the carboxylate ligand evolved from the CO_2 π_{ip}* orbital is doubly occupied, which indicates that the 2 e reduction of CO_2 is nearly completed.

The last step of the reaction consists of breaking the C−O single bond in ^{3}**5** to generate the final product, CO. Several feasible reaction pathways have been investigated since C−O bond cleavage has been shown to be the rate-determining step for CO_2 reduction by [Re(bpy)(CO)$_3$].[19b] Our calculations reveal that the occurrence of direct hydroxide dissociation is impossible, although we did not succeed in locating the associated transition state. In fact, upon carrying out a series of relaxed surface scans as a function of the cleaving C−O bond distance, it turns out that the energy consistently increases by up to 36 kcal/mol as the C−O bond lengthens. To compensate for the energetic penalty arising from C−O bond cleavage, the C−O bond scission should couple with the formation of another bond. On the triplet surface the transformation of ^{3}**5** to ^{3}**6** is computed to involve rather low barriers if the reaction is assisted by H_3O^+ (0 kcal/mol) or H_2CO_3 (2.8 kcal/mol, pK_{a1} = 3.6). The transition-state geometry of the latter (Supporting Information, Figure S2) suggests that C−O bond breaking is concerted with O−H bond formation, which verifies the thermodynamic argument. The barrier increases to 12.6 kcal/mol if H_2O, a much weaker Brönsted acid, is invoked. If the reference point is chosen to be the infinitely separated reactants, the barrier becomes 20.9 kcal/mol. This value is comparable to the corresponding barrier (22.5 kcal/mol[19b]) computed for CO_2 activation by [Re(bpy)(CO)$_3$] with CH_3OH (pK_a = 15.5 in water) serving as the proton source. However, the ground state of **6** is computationally predicted to be a singlet with a triplet/singlet energy separation of 4.9 kcal/mol, and the located minimum energy crossing point between ^{3}**6** and ^{1}**6** is situated only 2.2 kcal/mol higher in energy above ^{3}**6**. In comparison with the larger triplet-singlet gap of **5** (14.4 kcal/mol), one can conclude that the C−O bond cleavage of ^{3}**5** prevails on the triplet surface, which is followed by spin-crossover to yield ^{1}**6**. Thus, the C−O bond breaking is facile in the presence of H_3O^+ or H_2CO_3 and hence is effectively concerted with the preceding PCET. A similar mechanism has been proposed for the CO_2 reduction by Fe(porphyrin) systems.[41]

Our calculations suggest that CO adduct ^{1}**6** may either directly release CO with a moderate free energy decrease of 5.7 kcal/mol or easily accept another electron to form ^{2}**7** as the computed 1 e reduction potential of ^{1}**6** (−0.32 V) is more positive than −1.21 V. In contrast with the exergonic CO release process starting from ^{1}**6**, the CO dissociation from ^{2}**7** is endergonic by 8.6 kcal/mol, in accord with the fact that CO as a typical π-acid ligand binds more strongly with an electron-rich metal. Thus, the CO release is likely to happen after the generation of ^{1}**6**, and ^{2}**7** may be accumulated during the catalysis. The latter prediction is indeed the case since ^{2}**7** has been experimentally identified to be an intermediate in the catalytic cycle.[6b,42] On the other hand, one may argue that free CO can readily recombine with ^{2}**1** to generate ^{2}**7** and hence poison the catalyst; however, the limited solubility in water of CO (27.6 mg/L)[43] compared with that of CO_2 (1.5 g/L)[43] considerably lowers the probability of such process. Nevertheless, to some extent this leads to the accumulation of ^{2}**7** as well.

Taken together, our theoretical results predict that once the CO_2 adduct forms, the subsequent transformation is reasonably facile in the presence of efficient proton donors. With respect to the overall mechanism, the overpotential originates from the formation of the potent nucleophile ^{2}**1**, which is able to

dx.doi.org/10.1021/ic500829p | Inorg. Chem. 2014, 53, 7500−7507

efficiently donate electrons into the high-energy CO_2 π^* orbital. To decrease the overpotential, one may suggest modification of the ligand in a way that would enhance the stability of Ni^I species. However, such modifications might lower the CO_2 affinity of Ni^I complexes that have more positive reduction potentials. For instance, the 1 e reduction waves of $[Ni^{II}(DMC)]^{2+}$ and $[Ni^{II}(TMC)]^{2+}$ appear at −1.03 and −0.65 V, respectively.[9] Our calculations show that CO_2 coordination to $[Ni(DMC)]^+$ is moderately endergonic by 5.2 kcal/mol, and that the CO_2 adduct of $[Ni(TMC)]^+$ cannot form. This could be due to the diminished reducing power of the Ni^I species and the increased steric crowding resulting from the substituents. Moreover, this may explain the attenuated reactivity of the CO_2 reduction by the Ni(cyclam) derivatives observed experimentally.[9] For future ligand design one must consider these two competing factors (overpotential vs CO_2 affinity). In fact, in the case of ^{2}**1**, the estimated binding free energy of CO_2 is close to zero; therefore, ^{2}**2** is in a fast equilibrium with CO_2 in solution. To increase the stability of CO_2 adducts, addition of Lewis acids or weak Brönsted acids is likely to be a method of choice, because the interaction of CO_2 with acids may facilitate the electron transfer from the metal center to CO_2 and hence strengthen the bonding between them.[15b,41]

Another limitation of the catalytic activity may arise from the low concentrations of the efficient proton donors ($[H_3O^+]$ = 0.15 mM and $[H_2CO_3]$ = 0.09 mM). In this regard, addition of weak Brönsted acids might speed up the reaction.[19a] To circumvent H_2 evolution, weak Brönsted acids with similar or slightly greater acidity than H_2CO_3 are the best targets for future experimental investigations.

SUMMARY

This work addresses a detailed computational study on homogeneous CO_2 reduction by Ni(cyclam). Our calculations reveal that formation of an η^1-CO_2 adduct is energetically favored by 14.0 kcal/mol relative to η^1-OCO. As a result, the proposed reaction pathway resulting in formate is blocked at the onset of the reaction. This elegantly explains the product selectivity that is observed experimentally. In the presence of efficient proton donors, further CO_2 functionalization is facile and likely proceeds via concerted proton−electron transfer and C−O bond cleavage. On the basis of the theoretical results, the limitations of the catalytic activity of Ni(cyclam) are also discussed, which provides more insights into future work in designing more efficient catalysts.

ASSOCIATED CONTENT

Supporting Information

Listings of the details about calculation of redox potentials and pK_a values, the details about the calculations of $[H_3O^+]$, $[H_2CO_3]$, and the related species in the mixed solvent, the details about the calculations of redox potentials under the experimental conditions, calculated reduction potentials by COSMO-RS (Table S1), relative energies of $[Ni(cyclam)]^+$ with different cyclam conformations (Table S2), space filling models of CO_2 adducts (Figure S1), the structure of the transition state associated with the C−O bond cleavage with H_2CO_3 being the proton donor (Figure S2), key MOs for *trans*-III $[Ni(cyclam)(CO_2)]^+$ (Figure S3), the reaction profile for *trans*-III $[Ni(cyclam)]^+$ (Figure S4), the reaction profile for formate formation starting from ^{2}**2′** (Figure S5), the reaction profile for H_2 evolution (Figure S6) and the coordinates of all intermediates. This material is available free of charge via the Internet at http://pubs.acs.org.

AUTHOR INFORMATION

Corresponding Author

*E-mail: shengfa.ye@cec.mpg.de.

Notes

The authors declare no competing financial interest.

ACKNOWLEDGMENTS

We are indebted to Drs. B. Mondal and M. Sparta for fruitful discussions and gratefully acknowledge financial support from the Max-Planck Society.

REFERENCES

(1) Tans, P.; Keeling, R. NOAA/ESRL (www.esrl.noaa.gov/gmd/ccgg/trends/) and Scripps Institution of Oceanography (scrippsco2.ucsd.edu/) (accessed June, 5, 2014).

(2) Aresta, M. *Carbon Dioxide as Chemical Feedstock;* Wiley-VCH Verlag GmbH & Co. KGaA: Weinheim, Germany, 2010; pp 9−11.

(3) Benson, E. E.; Kubiak, C. P.; Sathrum, A. J.; Smieja, J. M. *Chem. Soc. Rev.* **2009**, *38*, 89−99.

(4) (a) Costentin, C.; Robert, M.; Savéant, J.-M. *Chem. Soc. Rev.* **2013**, *42*, 2423−2436. (b) Schneider, J.; Jia, H.; Muckerman, J. T.; Fujita, E. *Chem. Soc. Rev.* **2012**, *41*, 2036−2051. (c) Collin, J. P.; Sauvage, J. P. *Coord. Chem. Rev.* **1989**, *93*, 245−268. (d) Jitaru, M.; Lowy, D. A.; Toma, M.; Toma, B. C.; Oniciu, L. *J. Appl. Electrochem.* **1997**, *27*, 875−889. (e) Qiao, J.; Liu, Y.; Hong, F.; Zhang, J. *Chem. Soc. Rev.* **2014**, *43*, 631−675. (f) Aresta, M.; Dibenedetto, A.; Angelini, A. *Chem. Rev.* **2014**, *114*, 1709−1742. (g) Appel, A. M.; Bercaw, J. E.; Bocarsly, A. B.; Dobbek, H.; DuBois, D. L.; Dupuis, M.; Ferry, J. G.; Fujita, E.; Hille, R.; Kenis, P. J.; Kerfeld, C. A.; Morris, R. H.; Peden, C. H.; Portis, A. R.; Ragsdale, S. W.; Rauchfuss, T. B.; Reek, J. N.; Seefeldt, L. C.; Thauer, R. K.; Waldrop, G. L. *Chem. Rev.* **2013**, *113*, 6621−58. (h) Windle, C. D.; Perutz, R. N. *Coord. Chem. Rev.* **2012**, *256*, 2562−2570. (i) Inglis, J. L.; MacLean, B. J.; Pryce, M. T.; Vos, J. G. *Coord. Chem. Rev.* **2012**, *256*, 2571−2600. (j) Fan, T.; Chen, X.; Lin, Z. *Chem. Commun.* **2012**, *48*, 10808−10828. (k) Wang, W.; Wang, S.; Ma, X.; Gong, J. *Chem. Soc. Rev.* **2011**, *40*, 3703−3727. (l) Cokoja, M.; Bruckmeier, D.-C. C.; Rieger, B.; Herrmann, W. A.; Kühn, F. E. *Angew. Chem., Int. Ed.* **2011**, *50*, 8510−8537. (m) Whipple, D. T.; Kenis, P. J. A. *J. Phys. Chem. Lett.* **2010**, *1*, 3451−3458. (n) Takeda, H.; Ishitani, O. *Coord. Chem. Rev.* **2010**, *254*, 346−354. (o) Riduan, S. N.; Zhang, Y. *Dalton Trans.* **2010**, *39*, 3347−3357. (p) Mikkelsen, M.; Jørgensen, M.; Krebs, F. C. *Energy Environ. Sci.* **2010**, *3*, 43−81. (q) Grills, D. C.; Fujita, E. *J. Phys. Chem. Lett.* **2010**, *1*, 2709−2718. (r) Federsel, C.; Jackstell, R.; Beller, M. *Angew. Chem., Int. Ed.* **2010**, *49*, 6254−6257. (s) Doherty, M. D.; Grills, D. C.; Muckerman, J. T.; Polyansky, D. E.; Fujita, E. *Coord. Chem. Rev.* **2010**, *254*, 2472−2482. (t) Darensbourg, D. J. *Inorg. Chem.* **2010**, *49*, 10765−10780. (u) Costentin, C.; Robert, M.; Savéant, J.-M. *Chem. Rev.* **2010**, *110*, PR1−PR40. (v) Morris, A. J.; Meyer, G. J.; Fujita, E. *Acc. Chem. Res.* **2009**, *42*, 1983−1994. (w) Ma, J.; Sun, N.; Zhang, X.; Zhao, N.; Xiao, F.; Wei, W.; Sun, Y. *Catal. Today* **2009**, *148*, 221−231. (x) Savéant, J.-M. *Chem. Rev.* **2008**, *108*, 2348−2378. (y) Sakakura, T.; Choi, J.-C.; Yasuda, H. *Chem. Rev.* **2007**, *107*, 2365−2387. (z) Gattrell, M.; Gupta, N.; Co, A. *Energy Convers. Manage.* **2007**, *48*, 1255−1265. (aa) Omae, I. *Catal. Today* **2006**, *115*, 33−52. (ab) Gattrell, M.; Gupta, N.; Co, A. *J. Electroanal. Chem.* **2006**, *594*, 1−19. (ac) Jessop, P. G.; Joó, F.; Tai, C.-C. *Coord. Chem. Rev.* **2004**, *248*, 2425−2442. (ad) Dell'Amico, D. B.; Calderazzo, F.; Labella, L.; Marchetti, F.; Pampaloni, G. *Chem. Rev.* **2003**, *103*, 3857−3898. (ae) Leitner, W. *Acc. Chem. Res.* **2002**, *35*, 746−756. (af) Arakawa, H.; Aresta, M.; Armor, J. N.; Barteau, M. A.; Beckman, E. J.; Bell, A. T.; Bercaw, J. E.; Creutz, C.; Dinjus, E.; Dixon, D. A.; Domen, K.; DuBois, D. L.; Eckert, J.; Fujita, E.; Gibson, D. H.; Goddard, W. A.; Goodman, D. W.; Keller, J.; Kubas, G. J.; Kung, H. H.; Lyons, J. E.; Manzer, L. E.; Marks, T. J.; Morokuma, K.; Nicholas,

K. M.; Periana, R.; Que, L.; Rostrup-Nielson, J.; Sachtler, W. M. H.; Schmidt, L. D.; Sen, A.; Somorjai, G. A.; Stair, P. C.; Stults, B. R.; Tumas, W. *Chem. Rev.* **2001**, *101*, 953−996. (ag) Schneider, J.; Jia, H.; Kobiro, K.; Cabelli, D. E.; Muckerman, J. T.; Fujita, E. *Energy Environ. Sci.* **2012**, *5*, 9502−9510.
(5) Angamuthu, R.; Byers, P.; Lutz, M.; Spek, A. L.; Bouwman, E. *Science* **2010**, *327*, 313−315.
(6) (a) Collin, J. P.; Jouaiti, A.; Sauvage, J. P. *Inorg. Chem.* **1988**, *27*, 1986−1990. (b) Beley, M.; Collin, J. P.; Ruppert, R.; Sauvage, J. P. *J. Am. Chem. Soc.* **1986**, *108*, 7461−7467. (c) Beley, M.; Collin, J.-P.; Ruppert, R.; Sauvage, J.-P. *J. Chem. Soc., Chem. Commun.* **1984**, 1315−1316.
(7) Kelly, C. A.; Mulazzani, Q. G.; Venturi, M.; Blinn, E. L.; Rodgers, M. A. J. *J. Am. Chem. Soc.* **1995**, *117*, 4911−4919.
(8) (a) Balazs, G. B.; Anson, F. C. *J. Electroanal. Chem.* **1993**, *361*, 149−157. (b) Balazs, G. B.; Anson, F. C. *J. Electroanal. Chem.* **1992**, *322*, 325−345.
(9) Froehlich, J. D.; Kubiak, C. P. *Inorg. Chem.* **2012**, *51*, 3932−3934.
(10) Koppenol, W. H.; Rush, J. D. *J. Phys. Chem.* **1987**, *91*, 4429−4430.
(11) Sutin, N.; Creutz, C.; Fujita, E. *Comments Inorg. Chem.* **1997**, *19*, 67−92.
(12) (a) Gibson, D. H. *Chem. Rev.* **1996**, *96*, 2063−2095. (b) Pandey, K. K. *Coord. Chem. Rev.* **1995**, *140*, 37−114. (c) Gambarotta, S.; Arena, F.; Floriani, C.; Zanazzi, P. F. *J. Am. Chem. Soc.* **1982**, *104*, 5082−5092. (d) Calabrese, J. C.; Herskovitz, T.; Kinney, J. B. *J. Am. Chem. Soc.* **1983**, *105*, 5914−5915. (e) Komiya, S.; Akita, M.; Kasuga, N.; Hirano, M.; Fukuoka, A. *J. Chem. Soc., Chem. Commun.* **1994**, 1115−1116. (f) Dohring, A.; Jolly, P. W.; Kruger, C.; Romao, M. J. *Z. Naturforsch., B: Chem. Sci.* **1985**, *40*, 484. (g) Aresta, M.; Nobile, C. F.; Albano, V. G.; Forni, E.; Manassero, M. *J. Chem. Soc., Chem. Commun.* **1975**, 636−637. (h) Anderson, J. S.; Iluc, V. M.; Hillhouse, G. L. *Inorg. Chem.* **2010**, *49*, 10203−10207. (i) Beck, R.; Shoshani, M.; Krasinkiewicz, J.; Hatnean, J. A.; Johnson, S. A. *Dalton Trans.* **2013**, *42*, 1461−1475. (j) Bristow, G. S.; Hitchcock, P. B.; Lappert, M. F. *J. Chem. Soc., Chem. Commun.* **1981**, 1145−1146. (k) Gambarotta, S.; Floriani, C.; Chiesi-Villa, A.; Guastini, C. *J. Am. Chem. Soc.* **1985**, *107*, 2985−2986. (l) Alvarez, R.; Carmona, E.; Marin, J. M.; Poveda, M. L.; Gutierrez-Puebla, E.; Monge, A. *J. Am. Chem. Soc.* **1986**, *108*, 2286−2294. (m) Field, J. S.; Haines, R. J.; Sundermeyer, J.; Woollam, S. F. *J. Chem. Soc., Dalton Trans.* **1993**, 2735−2748. (n) Wang, T.-F.; Hwu, C.-C.; Tsai, C.-W.; Lin, K.-J. *Organometallics* **1997**, *16*, 3089−3090. (o) Wang, T.-F.; Hwu, C.-C.; Wen, Y.-S. *J. Organomet. Chem.* **2004**, *689*, 411−418. (p) Castro-Rodriguez, I.; Nakai, H.; Zakharov, L. N.; Rheingold, A. L.; Meyer, K. *Science* **2004**, *305*, 1757−1759.
(13) (a) Sakaki, S.; Koga, N.; Morokuma, K. *Inorg. Chem.* **1990**, *29*, 3110−3116. (b) Dedieu, A.; Ingold, F. *Angew. Chem., Int. Ed. Engl.* **1989**, *28*, 1694−1695.
(14) Sakaki, S. *J. Am. Chem. Soc.* **1990**, *112*, 7813−7814.
(15) (a) Bhugun, I.; Lexa, D.; Savéant, J.-M. *J. Phys. Chem.* **1996**, *100*, 19981−19985. (b) Bhugun, I.; Lexa, D.; Savéant, J.-M. *J. Am. Chem. Soc.* **1996**, *118*, 1769−1776. (c) Bhugun, I.; Lexa, D.; Saveant, J.-M. *J. Am. Chem. Soc.* **1994**, *116*, 5015−5016. (d) Hammouche, M.; Lexa, D.; Momenteau, M.; Saveant, J. M. *J. Am. Chem. Soc.* **1991**, *113*, 8455−8466.
(16) Rakowski Dubois, M.; Dubois, D. L. *Acc. Chem. Res.* **2009**, *42*, 1974−1982.
(17) Hammes-Schiffer, S. *Energy Environ. Sci.* **2012**, *5*, 7696−7703.
(18) Fujita, E.; Szalda, D. J. *Inorg. Chim. Acta* **2000**, *297*, 139−144.
(19) (a) Smieja, J. M.; Sampson, M. D.; Grice, K. A.; Benson, E. E.; Froehlich, J. D.; Kubiak, C. P. *Inorg. Chem.* **2013**, *52*, 2484−2491. (b) Keith, J. A.; Grice, K. A.; Kubiak, C. P.; Carter, E. A. *J. Am. Chem. Soc.* **2013**, *135*, 15823−15829. (c) Smieja, J. M.; Benson, E. E.; Kumar, B.; Grice, K. A.; Seu, C. S.; Miller, A. J. M.; Mayer, J. M.; Kubiak, C. P. *Proc. Natl. Acad. Sci. U. S. A.* **2012**, *109*, 15646−15650. (d) Benson, E. E.; Sampson, M. D.; Grice, K. A.; Smieja, J. M.; Froehlich, J. D.; Friebel, D.; Keith, J. A.; Carter, E. A.; Nilsson, A.; Kubiak, C. P. *Angew. Chem., Int. Ed.* **2013**, *52*, 4841−4844. (e) Bourrez, M.; Molton, F.; Chardon-Noblat, S.; Deronzier, A. *Angew. Chem., Int. Ed.* **2011**, *50*, 9903−9906.
(20) Agarwal, J.; Shaw, T. W.; Stanton, C. J.; Majetich, G. F.; Bocarsly, A. B.; Schaefer, H. F. *Angew. Chem., Int. Ed.* **2014**, *53*, 5152−5155.
(21) Neese, F. *Wiley Interdiscip. Rev.: Comput. Mol. Sci.* **2012**, *2*, 73−78.
(22) Lee, C.; Yang, W.; Parr, R. G. *Phys. Rev. B* **1988**, *37*, 785−789.
(23) van Lenthe, E.; Baerends, E. J.; Snijders, J. G. *J. Chem. Phys.* **1993**, *99*, 4597−4610.
(24) (a) Pantazis, D. A.; Chen, X.-Y.; Landis, C. R.; Neese, F. *J. Chem. Theory Comput.* **2008**, *4*, 908−919. (b) Schäfer, A.; Horn, H.; Ahlrichs, R. *J. Chem. Phys.* **1992**, *97*, 2571−2577.
(25) (a) Neese, F.; Wennmohs, F.; Hansen, A.; Becker, U. *Chem. Phys.* **2009**, *356*, 98−109. (b) Kossmann, S.; Neese, F. *Chem. Phys. Lett.* **2009**, *481*, 240−243. (c) Izsák, R.; Neese, F.; Klopper, W. *J. Chem. Phys.* **2013**, *139*, 094111. (d) Izsák, R.; Neese, F. *J. Chem. Phys.* **2011**, *135*, 144105.
(26) Weigend, F. *Phys. Chem. Chem. Phys.* **2006**, *8*, 1057−1065.
(27) (a) Grimme, S.; Ehrlich, S.; Goerigk, L. *J. Comput. Chem.* **2011**, *32*, 1456−1465. (b) Grimme, S.; Antony, J.; Ehrlich, S.; Krieg, H. *J. Chem. Phys.* **2010**, *132*, 154104.
(28) (a) Xue, G.; Geng, C.; Ye, S.; Fiedler, A. T.; Neese, F.; Que, L., Jr. *Inorg. Chem.* **2013**, *52*, 3976−3984. (b) Ye, S.; Riplinger, C.; Hansen, A.; Krebs, C.; Bollinger, M., Jr.; Neese, F. *Chem.—Eur. J.* **2012**, *18*, 6555−6567.
(29) Connors, K. A. *Chemical Kinetics: The Study of Reaction Rates in Solution;* VCH: New York, 1990; pp 99−101.
(30) Weigend, F.; Ahlrichs, R. *Phys. Chem. Chem. Phys.* **2005**, *7*, 3297−3305.
(31) Klamt, A.; Schüürmann, G. *J. Chem. Soc., Perkin Trans. 2* **1993**, 799−805.
(32) (a) *Handbook of Chemistry & Physics,* 94th ed.; CRC Press: Boca Raton, FL, 2013−2014; pp 6−187. (b) Gagliardi, L. G.; Castells, C. B.; Ràfols, C.; Rosés, M.; Bosch, E. *J. Chem. Eng. Data* **2007**, *52*, 1103−1107.
(33) Kelly, C. P.; Cramer, C. J.; Truhlar, D. G. *J. Phys. Chem. B* **2006**, *111*, 408−422.
(34) Tawa, G. J.; Topol, I. A.; Burt, S. K.; Caldwell, R. A.; Rashin, A. A. *J. Chem. Phys.* **1998**, *109*, 4852−4863.
(35) (a) Baik, M.-H.; Friesner, R. A. *J. Phys. Chem. A* **2002**, *106*, 7407−7412. (b) Fu, Y.; Liu, L.; Yu, H. Z.; Wang, Y. M.; Guo, Q. X. *J. Am. Chem. Soc.* **2005**, *127*, 7227−7234.
(36) Klamt, A. *J. Phys. Chem.* **1995**, *99*, 2224−2235.
(37) Barefield, E. K.; Bianchi, A.; Billo, E. J.; Connolly, P. J.; Paoletti, P.; Summers, J. S.; Van Derveer, D. G. *Inorg. Chem.* **1986**, *25*, 4197−4202.
(38) Connolly, P. J.; Billo, E. J. *Inorg. Chem.* **1987**, *26*, 3224−3226.
(39) Sakaki, S. *J. Am. Chem. Soc.* **1992**, *114*, 2055−2062.
(40) Ye, S.; Geng, C.-Y.; Shaik, S.; Neese, F. *Phys. Chem. Chem. Phys.* **2013**, *15*, 8017−8030.
(41) Costentin, C.; Drouet, S.; Passard, G.; Robert, M.; Savéant, J.-M. *J. Am. Chem. Soc.* **2013**, *135*, 9023−9031.
(42) Kelly, C. A.; Mulazzani, Q. G.; Blinn, E. L.; Rodgers, M. A. J. *Inorg. Chem.* **1996**, *35*, 5122−5126.
(43) *Handbook of Chemistry & Physics,* 94th ed.; CRC Press: Boca Raton, FL, 2013−2014; pp 5−161.